Journal of Solid State Chemistry 183 (2010) 1645–1651

Contents lists available at ScienceDirect

Journal of Solid State Chemistry

journal homepage: www.elsevier.com/locate/jssc

Structural characterization and thermal properties of polyamide 6.6/Mg, Al/adipate-LDH nanocomposites obtained by solid state polymerization

M. Herrero [a], P. Benito [a], F.M. Labajos [a], V. Rives [a,*], Y.D. Zhu [b], G.C. Allen [b], J.M. Adams [c]

[a] GIR-QUESCAT-Departamento de Química Inorgánica, Universidad de Salamanca, 37008 Salamanca, Spain
[b] Interface Analysis Centre, University of Bristol, Bristol BS2 8BS, UK
[c] School of Engineering and Computer Science, University of Exeter, Exeter EX4 4QF, UK

ARTICLE INFO

Article history:
Received 14 February 2010
Received in revised form
11 May 2010
Accepted 12 May 2010
Available online 15 May 2010

Keywords:
Nanocomposites
Layered double hydroxide
Polyamide 6.6
Thermal properties
Solid state polymerization

ABSTRACT

A new nanocomposite was obtained by dispersing an adipate-modified layered double hydroxide (Ad-LDH) with adipic acid and hexamethylene diamine. These samples were polymerized in the solid phase under a nitrogen flow for 200 min at 190 °C. The structural and compositional details of the nanocomposite were determined by powder X-ray diffraction (PXRD), fourier transform infrared (FTIR) spectroscopy, focused ion beam (FIB), thermogravimetric analysis (TGA) and differential thermal analysis (DTA). The PXRD patterns and FIB images show a partially intercalated and partially exfoliated dispersion of layered crystalline materials in the polyamide 6.6 matrix. The best dispersion level is achieved in polyamide 6.6/LDH nanocomposites with low LDH loading. Some residual tactoids and particle agglomerates are also evident at high concentration. The best thermal stability of the nanocomposites is shown by the sample with 0.1% LDH content, for which it is higher than that of pure polyamide.

1. Introduction

In recent years, the dispersion of low loadings (ca. 5%) of inorganic particles in the nanosize scale in organic polymers is a challenge for the preparation of new composite materials with enhanced mechanical, gas barrier and flame retardant properties, when compared to those of composites prepared with micron size particles [1,2]. A homogeneous dispersion of nanoparticles is believed to contribute better to the property improvement.

Although fillers like alumina, silica, etc., can be added, layered inorganic compounds possess unique properties to be active as fillers in polymeric nanocomposites. They can be, in fact, exfoliated into single layers, each of them having a thickness of the order of nanometers (from ca. 0.7 to 2.5 nm) and by ion exchange or grafting reactions the surface of the layers may be functionalized with organic groups that increase the compatibility with the polymers [3]. In addition, layered solids may intercalate polymeric chains in their interlayer regions. Until now, however, the clay materials involved in this field have been mostly focused on montmorillonite-type layered silicates whose layers have a relatively low charge density and from which exfoliated montmorillonite-type layered silicate/polymer nanocomposites can be easily obtained [4–6]. However, scarce attention has been paid to anionic layered inorganic materials of the hydrotalcite type, even if these latter materials compare favourably with natural clays in terms of purity, control of crystallinity and particle size, and wider possibility of functionalization [7–10].

Hydrotalcite-like compounds, also known as layered double hydroxides (LDHs), are brucite-like layered materials, with hydrated anionic counterions in the gallery space [11–13]. The positive layer charge is originated by the partial isomorphic substitution of divalent cations by trivalent ones. In order to attain electroneutrality, an appropriate number of anions must be incorporated into the interlamellar domain. Their general chemical formula is $[M^{2+}_{1-x}M^{3+}_{x}(OH)_2]^{x+}A^{m-}_{x/m}\cdot nH_2O$, where M^{2+} is a divalent cation, M^{3+} is a trivalent cation and A is an interlamellar anion with formal charge m^-. The identities of M^{2+}, M^{3+} and of the interlayer anion, together with the value of the stoichiometric coefficient (x), may be varied over a wide range, giving rise to a large class of isostructural materials. This flexibility in composition allows preparing LDHs with a wide variety of properties [14], finding a wide range of applications; they can be used as catalysts or catalyst supports, anion exchangers, polymer stabilizers, etc. [2,15,16]. When these materials are to be used as hydrophobic polymer filler, pristine LDHs is not suitable and the insertion of anionic organic species with a long hydrophobic tail is necessary, which on one hand causes the expansion of the interlayer distance and on the other makes the LDH materials more compatible with organic polymers [2,17].

Several methods have been developed to produce clay/polymer nanocomposites [1,18,19]. Three methods were developed in the early stages of this field and have been applied widely. These are: *in situ* polymerization [20,21,22], solution induced

* Corresponding author. Fax: +34 923294574.
E-mail address: vrives@usal.es (V. Rives).

0022-4596/$ - see front matter © 2010 Elsevier Inc. All rights reserved.
doi:10.1016/j.jssc.2010.05.014

intercalation [23,24], and melt processing [25]. The most appropriate method, in order to produce well-exfoliated nanocomposites, is the *in situ* polymerization. This method consists in swelling the inorganic material by the monomer, followed by polymerization initiated well thermally or by addition of a suitable catalyst [3]. The chain growth in the interlayer space accelerates particle exfoliation and composite formation. This technique is also particularity attractive due to its versatility and compatibility with reactive monomers and is beginning to be used for commercial applications [26]. *In situ* intercalation polymerization enables significant control over both the polymer architecture and the final structure of the composite [27].

In a previous paper, we reported the synthesis of the intercalated nanocomposite based on Mg, Al-adipate LDH and polyamide 6.6 [28] through the solid state polymerization (SSP) method [29]. Previously to the SSP, polyamide 6.6 salt (PA6.6sal), a low molecular weight condensate, was obtained by a stoichiometric stepwise reaction between adipic acid (AA) and hexametilenediamine (HMDA). In such condensation process, there is an equilibrium such as: AA+HMDA↔PA6.6 salt+H_2O [29]. Polyamide 6.6 is an important semi-crystalline engineering polymer widely used due to its combination of properties such as high stiffness and strength at elevated temperatures, toughness, good abrasion and wear resistance, coupled with an excellent short term heat resistance due to its high melting point of ~260 °C [30]. The morphology and dispersion of LDH particles in LDH/PA6.6 sal nanocomposites were investigated using focused ion beam (FIB) techniques, transmission electron microscopy (TEM) and X-ray diffraction (XRD). In this paper, the samples characterization has been completed, the interactions between LDH and PA6.6 were discussed by FTIR spectroscopy and the thermal stability was determined by TG and DTA analyses.

2. Experimental

2.1. Materials and preparation of the organomodified-LDH

The reagents, $Mg(NO_3)_2 \cdot 6H_2O$, $Al(NO_3)_3 \cdot 9H_2O$, NaOH, adipic acid (AA) and hexamethylene diamine (HMDA), were from Panreac (Spain). All of them were used without further purification.

A Mg–Al LDH with Mg:Al molar ratio 2 (Mg,Al/Ad) with adipate (Ad) in the interlayer was prepared by the co-precipitation method at a constant pH [31]. A solution (solution A) was prepared by dissolving $Mg(NO_3)_2 \cdot 6H_2O$ and $Al(NO_3)_3 \cdot 9H_2O$ in 250 mL of water with a total Mg/Al concentration of 0.6 mol/L. A second solution (solution B) was prepared by dissolving NaOH in 800 mL of water (NaOH concentration 1 mol/L). A third solution (solution C) was prepared by dissolving AA in 100 mL water; the quantity of AA used was twice the anionic exchange capacity of the LDH (i.e. AA/Al molar ratio=2). Solution C was neutralized directly in the 3-neck vessel used for the synthesis by adding solution B until a pH=10 was reached. Solutions A and B were added drop-wise to solution C with intense stirring, the pH being maintained at a value of 10.0. Addition was completed in 4 h. The slurry was aged, in order to obtain well crystallized and uniform particle size distribution, for 3 h at 125 °C in a microwave oven. The microwave–hydrothermal experiments were carried out in a Milestone Ethos Plus microwave oven where reactants were treated in teflon liners. The microwave oven used a 2.45 GHz frequency radiation and the power supplied was that necessary to attain the temperature previously programmed. In order to minimize contamination with atmospheric CO_2, the preparation of this compound (Ad-LDH) was carried out under a nitrogen purge.

2.2. Preparation of LDH/PA6.6 nanocomposites

The nanocomposites were prepared by *in situ* intercalative polymerization, following a method similar to those used on a laboratory scale to prepare polyamide 6.6 [32,33]. A given amount of HMDA and AA with a molar ratio 1 was added to 50 mL of Ad-LDH slurry. The mixture was refluxed under nitrogen for 3 h at 100 °C. Several mixtures with different LDH/polymer ratios (0%, 0.1%, 0.5%, 1%, 2% and 5%, mass fraction of LDH content) were prepared. Then, the polyamide 6.6 salts were obtained by recrystallization upon vaporization of water.

In order to polymerize the monomer, the samples were heated under an inert atmosphere for 200 min at 190 °C. The temperature was chosen because it is in the vicinity of the melting point of the polyamide salt, to avoid thermal decomposition [34].

The formulations (0.1%, 0.5%, 1%, 2% and 5%) were chosen because no improvements were obtained on using higher LDH loading by *in situ* polymerization. The samples are named as *X*PA6.6, where *X* is the weight concentration of LDH.

2.3. Characterization and measurements

Powder X-ray diffraction (PXRD) patterns were recorded in a Siemens D-500 instrument using Cu-*K*α radiation (λ=1.54050 Å) and equipped with Diffract AT software. Identification of the crystalline phases was made by comparison with the JCPDS files [35].

The FTIR spectra were recorded in a Perkin-Elmer FT1730 instrument, using KBr pellets; 100 spectra (recorded with a nominal resolution of 4 cm^{-1}) were averaged to improve the signal-to-noise ratio.

Thermogravimetric (TG) and differential thermal analyzes (DTA) were carried out in TG-7 and DTA-7 instruments from Perkin-Elmer, in flowing oxygen or nitrogen (from L'Air Liquide, Spain), respectively, at a heating rate of 10 °C min^{-1}.

An FEI FIB201 gallium focused ion beam (FIB) instrument was used for sectioning and high-resolution imaging.

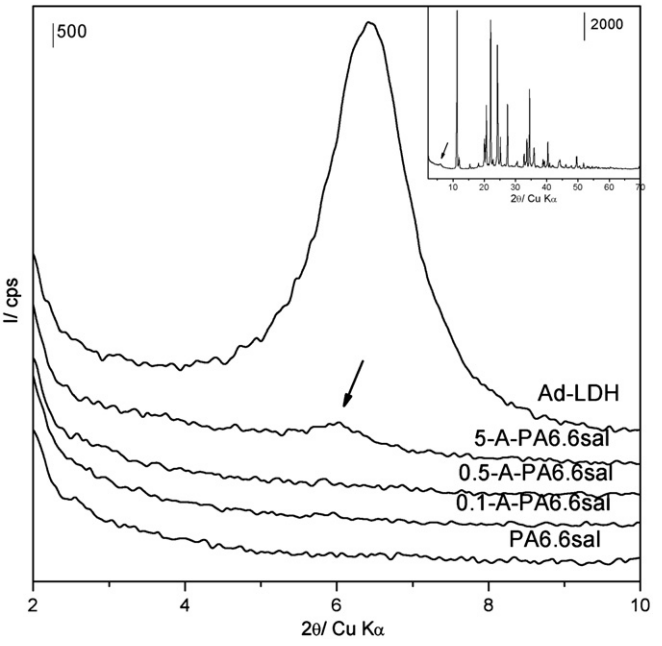

Fig. 1. Powder X-ray diffraction patterns of Mg, Al/Ad-LDH, 5PA6.6 sal, 0.5PA6.6 sal, 0.1PA6.6 sal and PA6.6 sal. Inset: full range diagram for sample 5PA6.6 sal. The arrows indicate the expected position for diffraction by (003) planes of hydrotalcite.

3. Results and discussion

Fig. 1 shows the PXRD patterns in the $2\theta=2$–10° range for the Mg, Al/Ad-LDH sample (Ad-LDH), the polymer sample (PA6.6sal), and several different polyamide 6.6/Ad-LDH nanocomposites (XPA6.6 sal, $x=0.1$, 0.5, 1, 2, 5). The basal spacings of Ad-LDH were calculated by the Bragg equation from the positions of (00l) peaks using the average value $[1/3][d_{003}+2d_{006}+3d_{009}]$. The basal spacing value ≈ 14 Å is similar to those reported previously for hydrotalcite-like compounds containing adipate oriented with the main plane of the carboxylate anions perpendicular to the brucite-like layers [36,37]. The large space between the Mg/Al nanolayers should promote the intercalation of a polymer, leading to an easy exfoliation of the stacked Mg/Al nanolayers in the polymer matrix to yield polyamide 6.6/LDH nanocomposites [38].

The PXRD patterns of the sample containing 5% of Ad-LDH previously to polymerization (5PA6.6 sal) shows a weak diffraction maximum at $2\theta=6.05^\circ$, due to the LDH (Fig. 1). The presence of this weak peak suggests formation of small LDH aggregates. However, the amount of undispersed (or unexfoliated) LDH should be still rather small, as no other diffraction peak due to the LDH is recorded [39]. When the Ad-LDH content decreases (2%, 1%, 0.5% and 0.1%), the d_{00l} diffraction peak disappears completely. These percentages are rather low and the solids can be hardly detected by PXRD. Moreover, dispersion of the inorganic filler, as well as the possible exfoliation of the layers, should give rise to extremely low particles, unable to produce a coherent diffraction strong enough to be detected.

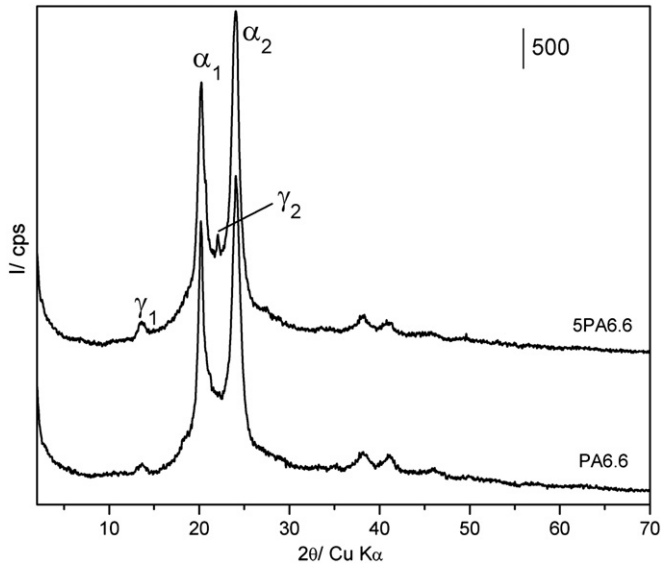

Fig. 2. Powder X-ray diffraction patterns of PA6.6 and 5PA6.6 nanocomposite.

The PXRD patterns of samples PA6.6 and 5PA6.6 after thermal treatment at 190 °C for 200 min in an inert atmosphere are included in Fig. 2. They show two strong diffraction peaks due to polyamide 6.6 at $2\theta=19.7$ and 23.2°, which are assigned to diffraction by (100) and (010, 110) planes, respectively [40]. These are distinctive features of the α-form crystal of polyamide 6.6, and the diffraction can be indexed to a simple one-chain triclinic unit cell [41,42]. Peak α_1 in the PXRD pattern of polyamide 6.6 arises from intrasheet hydrogen bonding, while the α_2 peak arises from intersheet hydrogen bonding [43]. Another very weak peak is registered for both samples at $2\theta=13.4^\circ$, and it is due to the γ phase (γ_1), with a pseudo-hexagonal structure. However, a new peak, around $2\theta=22.3^\circ$, is registered for the 5PA66 sample. This peak is also attributed to the γ form, peak γ_2.

The increase in intensity of the γ_1 peak and the appearance of peak γ_2 in sample 5PA6.6 indicates that the addition of the LDH disturbs the perfect arrangement of hydrogen bonded sheets of the α phase. Probably, the addition of hydrotalcite favours the formation of the γ crystalline phase, due to the interaction between hydrotalcite-like compounds layers and polymer chains.

The FTIR spectra for the 1PA6.6 sample, with and without thermal treatment, are included in Fig. 3. The results indicate that a polymeric polyamide has been obtained.

The spectrum of the sample prepared with polyamide 6.6 sal, i.e., without thermal treatment, shows broad and strong absorption bands at 2600–3000 cm^{-1} ($-NH_3^+$) and strong and sharp bands at 1648, 1516, 1402, 1383 cm^{-1} ($-COO^-$), which are characteristics of the ammonium salt of a carboxylic acid.

In the thermally treated samples, the characteristic band of the amide moiety, 3300 cm^{-1} (N–H stretching vibration) is also recorded; the band due to the ν(N–H) vibration, overlapped with the band due to the stretching mode of the lamellar hydroxyl

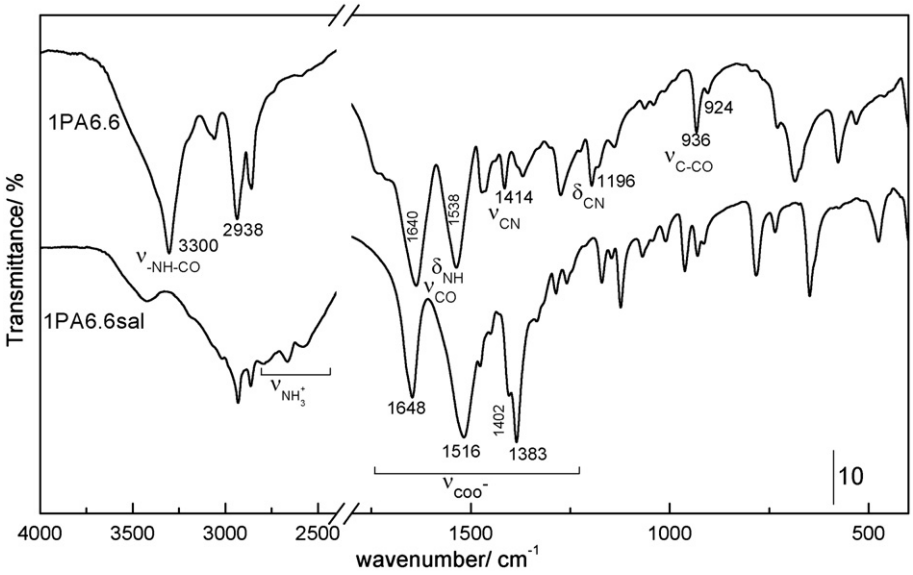

Fig. 3. FTIR spectra of sample 1PA6.6 nanocomposite with and without thermal treatment.

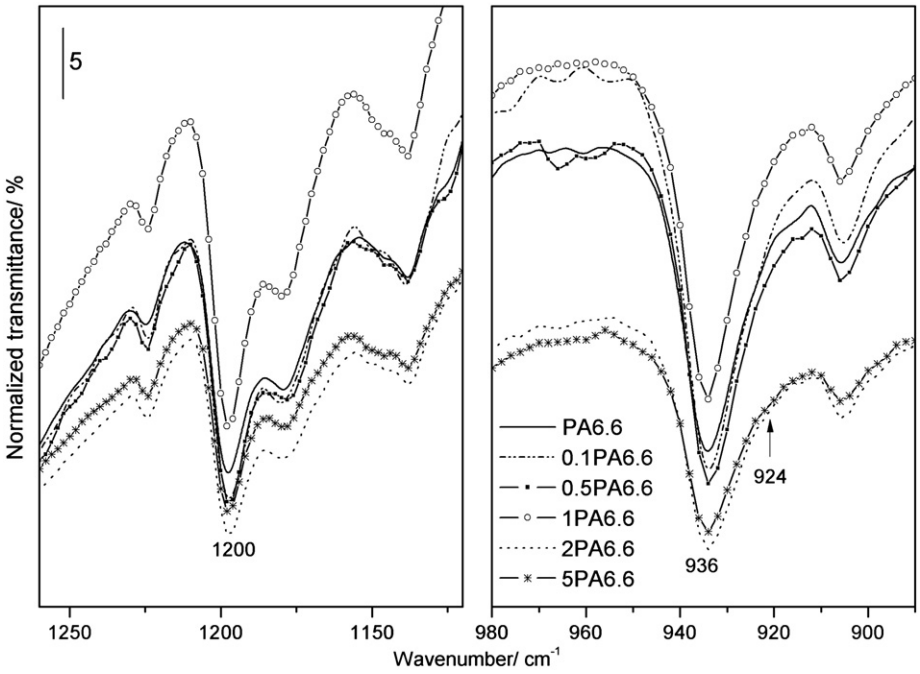

Fig. 4. FTIR spectra of PA6.6 and nanocomposites among the regions: 1260–1120 cm^{-1} (left) and 980–890 cm^{-1} (right). All spectra were normalized for comparison.

groups, is also observed. The ν (C=O) band is observed at ca. 1640 cm^{-1}, and the NH bending mode gives rise to the peak around 1538 cm^{-1}, which, together with the band at 1414 cm^{-1} (C–N stretching vibration) is characteristic of large polyamide 6.6 molecules. Other PA6.6 characteristic bands are also recorded, around 2938 cm^{-1} (CH_2 stretch), 1370 cm^{-1} (CN stretch+ in-plane NH deformation, amide III) and 1196 cm^{-1} (amide III coupled with hydrocarbon skeleton) [44,45].

FTIR spectroscopy is able to inform about short-range order, which depends on the coupling of a vibration mode to adjacent vibrations. In PA6.6 there are two types of ordered structures, i.e., ordered hydrogen bonds and *trans* conformation of methylene chains. These structures are associated to their characteristic bands, one around 1200 cm^{-1} related to hydrogen bonding, and another at ~936 cm^{-1} due to the *trans* conformation of methylene chains [46]. Additionally, the *trans* conformer in the amorphous phase is responsible for a shoulder around 924 cm^{-1} [47]. Consequently, the influence of the LDH content on hydrogen bonds and methylene stems in the crystalline state can be detected.

Fig. 4 depicts the effect of the LDH content on the bands of ordered and amorphous PA6.6. The spectra have been normalized for comparison. It can be observed that the bands at 936 and 1200 cm^{-1} become broader and weaker when the LDH content is increased, whereas the small shoulder at 924 cm^{-1} becomes stronger, even though it is difficult to resolve the band at 936 cm^{-1} and the shoulder at 924 cm^{-1}. This behaviour can suggest that the crystallinity of the sample decreases as a function of the LDH content.

Fig. 5 shows the TG curves of pure polyamide 6.6 and exfoliated 0.1PA6.6, 0.5PA6.6, 1PA6.6, 2PA6.6 nanocomposites. The thermal mass loss takes place in the 320–600 °C range. Three mass losses are observed for the parent polymer and the nanocomposites. The first mass loss (up to ca. 200 °C), corresponds to removal of water, the second (ca. 460 °C) to dehydroxylation and partial decomposition of the polymer, and the final step (above 460 °C) is due to oxidative elimination of the carbonaceous residue derived from the initial polymer degradation [48].

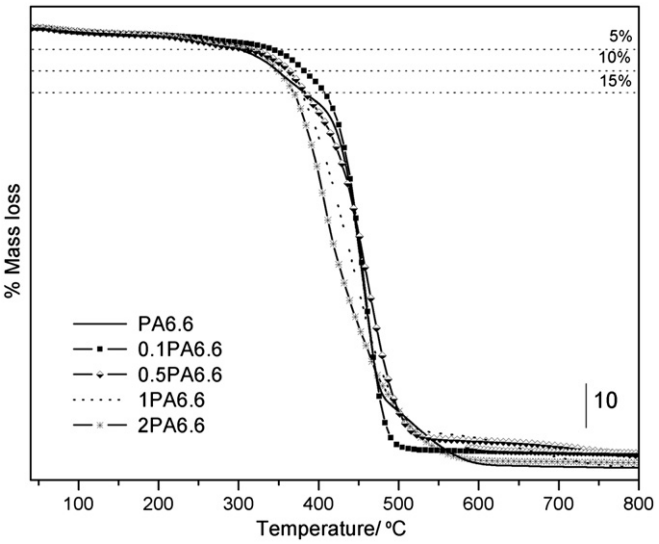

Fig. 5. TG analysis of some representative samples.

Fig. 6 shows the effect of LDH content on the thermal decomposition temperature at 5%, 10% and 15% mass loss. This figure shows that the decomposition temperature in the nanocomposite with 0.1% LDH increases significantly compared to that for pristine PA6.6. When the filler content is further increased, a decrease in thermal stability, in comparison to sample 0.1PA6.6, is progressively noticed. This thermal behaviour is similar to that previously reported for different nanocomposites [23,49], and it was there explained by the relative extent of exfoliation/delamination processes as a function of the amount of organo-LDH. The results suggest that an excess of LDH in the polymer matrix might restrict the chain

mobility as much as disturbing the participation of the polymer chain in the crystallizable unit [42]. In our system the critical loading level is about 0.5 wt% of nanolayers or LDH particles.

These results suggest that the thermal stability of the exfoliated material is somewhat improved. The enhancement of the thermal stability of the nanocomposite may be ascribed to a decrease in oxygen availability and volatile degradation products permeability/diffusivity deriving from the barrier effect of the exfoliated Mg, Al hydroxide nanolayers in the polyamide matrix.

However, when the Ad-LDH content increases further (samples with 1%, 2%, and 5% of filler) the thermal degradation temperature decreases. This behaviour is due to the fact that the high content of Ad-LDH can catalyze the alkaline degradation of polyamide 6.6 [50], which therefore decreases the molecular weight of PA6.6 and thus causes the sample to burn more easily.

The DTA traces were recorded in nitrogen atmosphere in order to obtain more information about the thermal transitions occurred. The DTA of low loaded samples are shown in Fig. 7. Two endothermal transitions are registered. The first peak at ca. 253 °C is due to melting of crystalline polyamide 6.6, and the second peak at ca. 438 °C corresponds to thermal degradation of polyamide 6.6 [51]. These results are in agreement with the thermogravimetric analysis behaviour shown above.

Decomposition of sample 0.1PA6.6 occurs at a temperature 8 °C above that of pure polyamide 6.6. In the other samples, with higher LDH contents, the degradation of polyamide compounds occurs at lower temperatures, indicating a degree of mutual interaction between the existing phases [45]. These results show that a high LDH content decreases the thermal stability of polyamide, probably due to accelerated chain hydrolysis arising from water released from the decomposed layered double hydroxide.

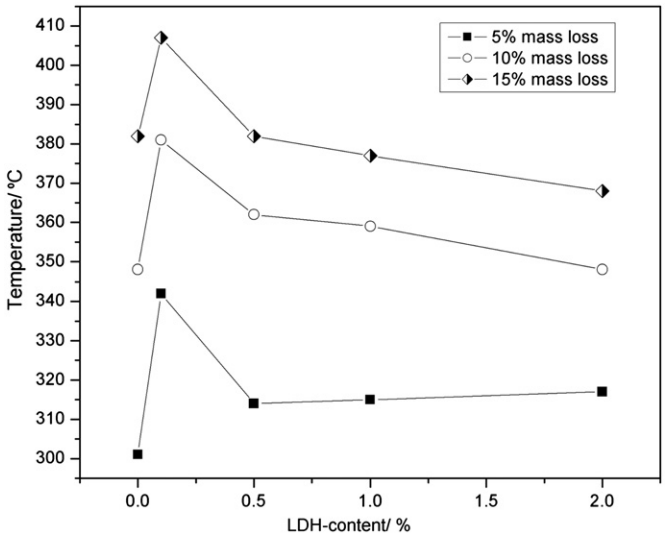

Fig. 6. Effect of LDH content on the decomposition temperature at 5%, 10% and 15% mass loss of nanocomposites.

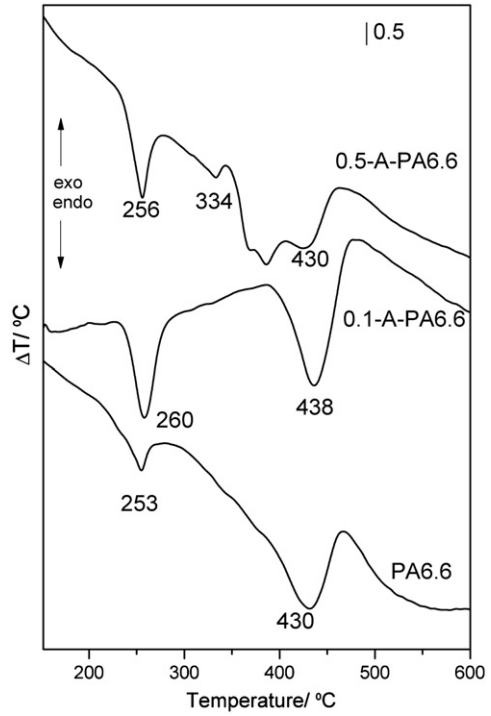

Fig. 7. DTA of PA6.6, 0.1PA6.6 and 0.5PA6.6 samples recorded in N_2 atmosphere.

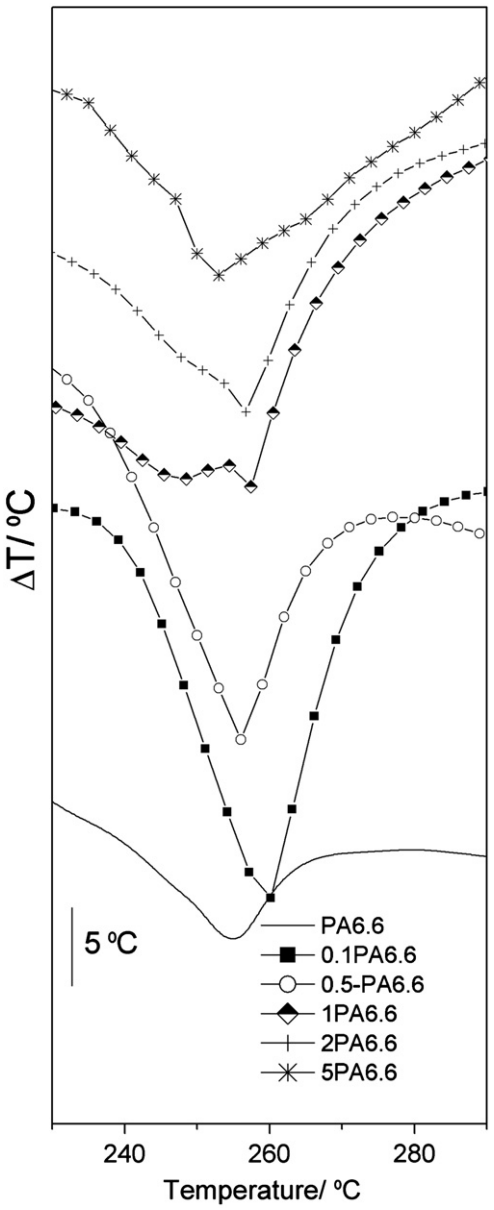

Fig. 8. DTA traces at PA6.6 and all nanocomposites in the range 230–290 °C.

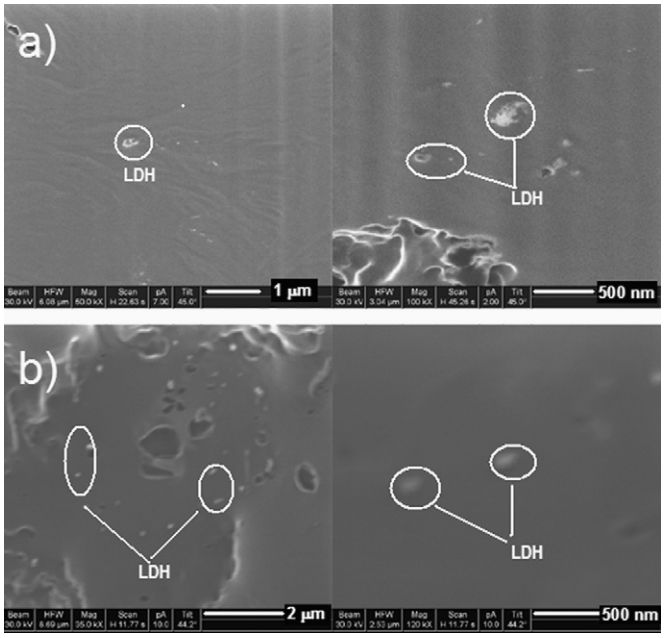

Fig. 9. FIB images of two representative nanocomposites samples at different LDH concentrations: (a) 1 PA6.6 and (b) 5 PA6.6 sal (left: low magnification, right: high magnification).

In order to evaluate the effect of LDH on the phase transition behaviour of polyamide 6.6, the melting point of PA6.6 and all nanocomposites have been measured, Fig. 8. Samples with high content of LDH show two melting peaks. According to some authors [52], this double melting phenomenon is due to a bimodal crystallite distribution of PA6.6. The high temperature melting peak has been attributed to the α form, while the low temperature one is due to the γ form [53]. These results indicate that the presence of a high content of LDH in the polymer matrix increases crystallization of the γ form. Therefore the presence of LDH increases the crystallization rate and has a strong effect on the heterophase nucleation of the PA6.6 matrix.

The FIB images for some representative nanocomposites samples containing 1% and 5% LDH are shown in Fig. 9. They show a disruption of ordered platelets, which indicates the presence of both intercalated layers and probably delaminated tactoids of LDH crystallites [28]. The tactoids are mostly in the form of thin platelets. It also should be noted that heat treatment has a little effect on the dispersion of LDH in the polyamide 6.6 matrix.

However, larger particles can also be observed and these may be residual undispersed tactoids. Tactoids of length greater than 140 nm are observed in the FIB images of all the polyamide 6.6/LDH nanocomposites samples, especially in the nanocomposites with higher LDH loadings. Furthermore, a few small agglomerates of LDH layers with variable thickness also appear in the nanocomposites. In this study, generally, the distribution of the LDH particles throughout the matrix appears inhomogeneous.

4. Conclusions

PA6.6/Ad-LDH composites have been synthesized by an *in situ* polymerization method. The nanodispersion of LDH in polyamide 6.6 may be qualitatively estimated from the analysis and PXRD patterns and FIB images. These show a partially intercalation and good dispersion of layered crystalline materials in the polyamide 6.6 (salt) matrix. The best dispersion level is achieved in low LDH-loaded nanocomposites. Some residual tactoids and particle agglomerates still exist at high concentration (5%). FTIR spectroscopy confirms that polymerization has taken place. The low LDH-loaded nanocomposites show a larger thermal stability than that of pure polyamide. When the 5%, 10% and 15% mass loss were selected as a comparison point, the decomposition temperature of 0.1PA6.6 was significantly higher than that of pure polyamide 6.6.

Acknowledgments

Authors thank financial support from MICINN (Grant MAT2009-08526) and ERDF.

References

[1] M. Alexandre, P. Dubois, Mater. Sci. Eng. 28 (2000) 1–63.
[2] L.A. Utracki, M. Sepehr, E. Boccaleri, Polym. Adv. Technol. 18 (2007) 1–37.
[3] F. Leroux, J.P. Besse, Chem. Mater. 13 (2001) 3507–3515.
[4] S. OLeary, D. O'Hare, G. Seeley, Chem. Commun. (2002) 1506–1507.
[5] P.C. LeBaron, Z. Wang, T.J. Pinnavaia, Appl. Clay Sci. 15 (1999) 11–29.
[6] G. Lagaly, Appl. Clay Sci. 15 (1999) 1–9.
[7] F. Leroux, J.P. Besse, in: F. Wypych, K.G. Satyanarayana (Eds.), Clay Surfaces: Fundamentals and ApplicationsElsevier Academic Press, London, 2004, pp. 459–495.
[8] F. Reny Costa, M. Saphiannikova, U. Wagenknecht, G. Heinrich, Adv. Polym. Sci. 210 (2008) 101–168.
[9] C. Taviot-Ghého, F. Leroux, in: X. Duan, D.G. Evans (Eds.), Layered Double Hydroxides, Structure and Bonding, vol. 119, Springer-Verlag, Berlin, 2006, pp. 121–159.
[10] F. Leroux, C. Taviot-Gueho, J. Mater. Chem. 15 (2005) 3628–3642.
[11] F. Trifiró, A. Vaccari, in: G. Alberti, T. Bein (Eds.), Comprehensive Supramolecular Chemistry, vol. 7, Pergamon, Elsevier Science, Oxford, 1996.
[12] V. Rives (Ed.), Layered Double Hydroxides: Present and FutureNova Science Publishers, Inc., New York, 2001.
[13] X. Duan, D.G. Evans (Eds.), Layered Double Hydroxides, Structure and Bonding, vol. 119, Springer-Verlag, Berlin, 2006.
[14] D.G. Evans, X. Duan, Chem. Commun. (2006) 485–496.
[15] M.R. Othmana, Z. Helwania, Martunus, W.J.N. Fernando, Appl. Organomet. Chem. 23 (2009) 335–346.
[16] D. Carriazo, M. Del Arco, C. Martín, V. Rives, Appl. Clay Sci. 37 (2007) 231–239.
[17] F.R. Costa, A. Leuteritz, U. Wagenknecht, D. Jehnichen, L. Häußler, G. Heinrich, Appl. Clay Sci. 38 (2008) 153–164.
[18] F. Gao, Mater. Today 11 (2004) 50–55.
[19] Q.H. Zeng, A.B. Yu, G.Q. Lu, D.R. Paul, J. Nanosci. Nanotechnol. 5 (2005) 1574–1592.
[20] G.A. Wang, C.C. Wang, C.Y. Chen, Polymer 46 (2005) 5065–5074.
[21] D.L. Lee, S.S. Im, J. Polym. Sci.: Polym. Phys. 45 (2007) 28–40.
[22] S. Martínez-Gallegos, M. Herrero, V. Rives, J. Appl. Polym. Sci. 109 (2008) 1388–1394.
[23] L. Qiu, W. Chen, B. Qu, Polymer 47 (2006) 922–930.
[24] L. Du, B. Qu, Y. Meng, Q. Zhu, Comput. Sci. Technol. 66 (2006) 913–918.
[25] W.D. Lee, S.S. Im, H.M. Lim, K.J. Kim, Polymer 47 (2006) 1364–1371.
[26] J.H. Chang, S.J. Kim, Y.L. Joo, S. Im, Polymer 45 (2004) 919–926.
[27] J.H. Chang, M.K. Mun, I.C. Lee, J. Appl. Polym. Sci. 98 (2005) 2009–2016.
[28] Y.D. Zhu, G.C. Allen, J.M. Adams, D. Gittins, M. Herrero, P. Benito, P.J. Heard, J. Appl. Polym. Sci. 108 (2008) 4108–4113.
[29] C.D. Papaspyrides, S.N. Vouyiouka, I.V. Blestos, Polymer 47 (2006) 1020–1027.
[30] R. Sengupta, S. Sabharwal, A.K. Bhowmick, T.K. Chaki, Polym. Degrad. Stab. 91 (2006) 1311–1318.
[31] W.T. Reichle, Solid State Ionics 22 (1986) 135–141.
[32] I.-Y. Wan, J.E. McGrath, T. Kashiwagi, in: G.L. Nelson (Ed.), ACS Symposium Series 599, American Chemical Society Washington, DC, 1995. pp. 29–40.
[33] K. Winnaker, E. Weingaertner, Tecnología Química, T.4, Editorial Gustavo Gili, S.A., Barcelona, 1958.
[34] L. Lei, N. Huang, Z. Liu, Z. Tang, W. Yung, Polym. Adv. Technol. 11 (2000) 242–249.
[35] JCPDS: Joint Committee on Powder Diffraction Standards, International Centre for Diffraction Data, Pennsylvania, USA, 1977.
[36] T. Hibino, A. Tsunashima, Chem. Mater. 9 (1997) 2082–2089.
[37] M. Herrero, F.M. Labajos, V. Rives, Appl. Clay Sci. 42 (2009) 510–518.
[38] H.-B. Hsueh, C.-Y. Chen, Polymer 44 (2003) 1151–1161.
[39] T.M. Wu, C.S. Liao, Macromol. Chem. Phys. 201 (2000) 2820–2825.
[40] K. Hedicke, H. Wittich, C. Mehler, F. Gruber, V. Altstädt, Comput. Sci. Technol. 66 (2006) 571–575.
[41] S.J. Cooper, M. Coogan, N. Everall, I. Priestnall, Polymer 42 (2001) 10119–10132.
[42] D.W. Chae, K.H. Lee, B.C. Kim, J. Polym. Sci. B 44 (2006) 371–377.
[43] N. Vasanthan, N.S. Murthy, R.G. Bray, Macromolecules 31 (1998) 8433–8435.

[44] L.J. Bellamy (Ed.), The Infra-Red Spectra of Complex Molecules, Wiley, New York, 1962, p. 174.
[45] R. Sengupta, A. Bandyopadhyay, S. Sabharwal, T.K. Chaki, A.K. Bhowmick, Polymer 46 (2005) 3343–3354.
[46] Y. Lu, Y. Zhang, G. Zhang, M. Yang, S. Yan, D. Shen, Polymer 45 (2004) 8999–9009.
[47] N. Vasanthan, D.R. Salem, J. Polym. Sci. B 38 (2000) 516–524.
[48] C.O. Oriakhi, I.V. Farr, M.M. Lerner, J. Mater. Chem. 6 (1996) 103–107.
[49] M.A. Paul, M. Alexandre, P. Degeé, C. Henrist, A. Rulmont, P. Dubois, Polymer 44 (2003) 443–450.
[50] L. Du, B. Qu, M. Zhang, Polym. Degrad. Stab. 92 (2007) 497–502.
[51] A. Licea-Claveríe, F.J.U. Carrillo, Polym. Testing 16 (1997) 445–453.
[52] P.R. Hornsby, J. Wang, R. Rothon, G. Wilkinson, K. Cossik, Polym. Degrad. Stab. 51 (1996) 235–249.
[53] T.-M. Wu, C.-S. Liao, Macromol. Chem. Phys. 201 (2000) 2820–2825.